Analyst

Cite this: *Analyst*, 2012, **137**, 1137

www.rsc.org/analyst

PAPER

Colorimetric quantification of galactose using a nanostructured multi-catalyst system entrapping galactose oxidase and magnetic nanoparticles as peroxidase mimetics†

Moon Il Kim,[a] Jongmin Shim,[b] Taihua Li,[a] Min-Ah Woo,[a] Daeyeon Cho,[c] Jinwoo Lee[b] and Hyun Gyu Park*[a]

Received 22nd September 2011, Accepted 14th December 2011
DOI: 10.1039/c2an15889b

A colorimetric method for quantification of galactose, which utilizes a nanostructured multi-catalyst system consisting of Fe_3O_4 magnetic nanoparticles (MNPs) and galactose oxidase (Gal Ox) simultaneously entrapped in large pore sized mesocellular silica, is described. Gal Ox, immobilized in a silica matrix, promotes reaction of galactose to generate H_2O_2 that subsequently activates MNPs in silica mesopores to convert a colorimetric substrate into a colored product. By using this colorimetric method, galactose can be specifically detected. Along with excellent reusability *via* application of simple magnetic capturing, enhanced operational stability was achieved by employing a cross-linked enzyme aggregate (CLEA) method for Gal Ox immobilization. This protocol leads to effective prevention of enzyme leaching from the pores of mesocellular silica. The analytical utility of the new colorimetric biosensor was demonstrated by its use in diagnosing galactosemia, a genetic metabolic disorder characterized by the inability to utilize galactose, through analysis of clinical dried blood spot specimens. A microscale well-plate format was employed that possesses a multiplexing capability. The multi-catalyst system entrapping Gal Ox and MNPs represents a new approach for rapid, convenient, and cost-effective quantification of galactose in human blood and it holds promise as an alternative method for galactosemia diagnosis, replacing the laborious procedures that are currently in use.

1. Introduction

Galactosemia is a group of inherited metabolic disorders characterized by enzyme deficiencies, which disrupt normal metabolism of galactose. Three types of galactosemia have been identified thus far.[1] These include type I associated with a deficiency of galactose-1-phosphate uridyl transferase (GALT), type II involving a deficiency of galactokinase (GALK), and type III connected with a deficiency of uridine diphosphate galactose-4-epimerase. Among this group, the most common and severest form of galactosemia is type I, termed as "classic galactosemia", which causes accumulation of galactose and galactose-1-phosphate in blood.[2] Galactosemia patients must carefully restrict their galactose intake from foods like milk and dairy products. Infants with galactosemia appear normal at birth, but serious symptoms such as liver dysfunction, cataracts, and kidney problems usually appear a few days after initiating milk intake unless properly treated.[3–5] Thus, early stage diagnosis of galactosemia in newborn babies, by determining the levels of galactose or galactose-1-phosphate in their blood or evaluating the activities of the three galactose-metabolizing enzymes, is critically needed. Due to its significance in human health, galactosemia is classified as one of the main metabolic disorders of newborn babies and, as a result, the diagnosis of this disease is currently mandatory and financially supported by governments of major countries including the USA and Korea.

The diagnosis of galactosemia is generally achieved by measuring galactose or galactose-1-phosphate concentrations using dried blood spot specimens to screen defects in the enzymes involved in galactose metabolism. For this purpose, several diagnostic methods have been developed. The most traditional one of these is a cell-based biological inhibition assay employing the method described by Guthrie[6] and Paigen.[7] However, this cell-based method can lead to erroneous results owing to the difficulty of consistently maintaining cell viability. The exact quantification of galactose concentrations at low levels is a challenging task. Procedures using instrumental methods, such as HPLC[8,9] and tandem mass spectrometry (MS/MS),[10] have also been used to rapidly determine galactose or

[a]*Department of Chemical and Biomolecular Engineering (BK21 Program), KAIST, Daejeon, 305-701, Republic of Korea. E-mail: hgpark@kaist.ac.kr; Fax: +82 42 350 3910; Tel: +82 42 350 3932*
[b]*Department of Chemical Engineering, POSTECH, Gyungbuk, 790-784, Republic of Korea*
[c]*Clinical Research Institute, Labgenomics, Seoul, 137-874, Republic of Korea*

† Electronic supplementary information (ESI) available. See DOI: 10.1039/c2an15889b

galactose-1-phosphate concentrations with high sensitivities. However, these techniques suffer from several drawbacks including the requirement of highly specialized instrumentation and complicated pre- or post-treatment methods, both of which lead to relatively high costs. An amperometric biosensor was developed by immobilizing Gal Ox in polyvinyl formal membrane for estimation of galactose in dairy products; however, the biosensor showed very limited linearity from 5 to 30 g L^{-1}, which is not applicable to determine galactose concentration at low levels like in the diagnosis of galactosemia.[11]

A microscale well-plate colorimetric assay, based on the coupled reactions catalyzed by alkaline phosphatase and galactose dehydrogenase, was recently developed.[12–14] In this assay, galactose is produced through the reaction of galactose-1-phosphate promoted by alkaline phosphatase and galactose dehydrogenase catalyzes the formation of NADH through oxidation of galactose by NAD^+. The resulting NADH activates diaphorase to convert iodonitrotetrazolium violet into the red colored product formazan, which can be detected colorimetrically. This method is both sensitive and quantitative, but its use of multiple components and complicated procedures could still limit its widespread use. Thus, a more advanced method for galactose quantification that overcomes the above-mentioned limitations is needed.

Recently, we described a new strategy, involving a multi-catalyst system comprised of glucose oxidase or cholesterol oxidase and MNPs as peroxidase mimetics, for achieving efficient colorimetric detection of target molecules.[15] The peroxidase activity of MNPs has been intensively utilized to develop novel colorimetric strategies to detect various biomolecules such as cell, protein, and carbohydrate.[16–18] In a continuing investigation in this area focusing on the development of practical clinical applications to the detection of galactose, we have developed a nanostructured multi-catalyst system that consists of MNPs and the oxidative enzyme Gal Ox simultaneously entrapped in mesoporous silica. In this effort, various analytical features of the new system, such as its selectivity, sensitivity, reusability, operational stability, and precision were assessed, and its clinical utility for galactosemia diagnosis using dried blood spot specimens derived from clinical samples was evaluated.

2. Experimental

2.1 Materials

2,2′-Azino-bis(3-ethylbenzo-thiazoline-6-sulfonic acid) diammonium salt (ABTS), glutaraldehyde (GA), galactose, glucose, arabinose, lactose, fructose, trichloroacetic acid and Gal Ox were purchased from Sigma-Aldrich (Milwaukee, WI), and 35% H_2O_2 was purchased from Junsei Chemical Co. (Japan). All other chemicals were at least analytical grade.

2.2 Characterization of synthetic materials

Transmission electron microscope (TEM) images were obtained on a Jeol EM-2010 microscope (Jeol Co.). N_2 adsorption/desorption isotherms at 77 K were performed using a micromeritics ASAP 2010 sorptometer (Micromeritics Co.). Powder X-ray diffraction (XRD) patterns were obtained with an 18 kW rotating anode X-ray generator (Rigaku Co.) and one-dimensional position sensitive detector (M. Braun Co.) using Cu Kα radiation ($\lambda = 1.5418$ Å) at a scanning rate of 4.00° min^{-1}. The dynamic light scattering (DLS) measurement of MMS-40 was performed on a Malvern particle size analyzer (Malvern, UK). To measure the diameter, MMS-40 (1 mL, 0.1 mg mL^{-1}) solution was placed in a polystyrene cuvette and scanned for 9 min (three runs) to obtain one set of raw data for the effective and most probable diameters. The average values for the diameters were determined with at least three repeated measurements per sample.

2.3 Synthesis of magnetic mesocellular silica (MMS)

Mesocellular silica was synthesized by modifying the reported procedure.[19] In a typical preparation, 9.8 g of triblock copolymer pluronic P123 was dissolved in 200 mL of water containing 4.4 mL of concentrated acetic acid. Subsequently, 5.9 g of 1,3,5-trimethylbenzene was added and the resulting mixture was heated to 60 °C with vigorous stirring for more than 2 h. Sodium silicate (16 mL) diluted with 200 mL of water was poured into the solution with vigorous stirring. The solution was reheated to 60 °C and aged for 20 h, followed by hydrothermal aging at 100 °C for 24 h. After calcination at 550 °C under air to remove block copolymers, mesocellular silica was obtained. To synthesize mesocellular silica impregnated with 40 wt% magnetite, 6.97 g of $Fe(NO_3)_3 \cdot 9H_2O$ was dissolved in 80 mL of ethanol, followed by addition of 2 g of mesocellular silica. The solution was stirred until the solvent had been evaporated and the resulting powder was heat-treated at 400 °C under a stream of argon (95%)/hydrogen (5%). The resulting sample was denoted as MMS-40. Mesocellular silica with 20 and 60 wt% magnetite were synthesized *via* the same procedure described above but using different amounts of $Fe(NO_3)_3 \cdot 9H_2O$ (2.62 and 15.69 g). The resulting samples were denoted as MMS-20 and MMS-60, respectively.

2.4 Preparation of the multi-catalyst system entrapping galactose oxidase in MMS

A mixture of MMS (10 mg) and 1.5 mL of Gal Ox (6 mg mL^{-1}) in a sodium phosphate buffer (10 mM, pH 6.5) was vortexed for 30 s, sonicated for 10 s, and incubated at room temperature with shaking (250 rpm). After 1 h incubation for adsorption of Gal Ox in MMS, the mixture was briefly washed with an aqueous buffer (100 mM sodium phosphate, pH 8.0), and incubated in the same buffer containing GA (0.1% w/w) at 200 rpm for 30 min. After GA treatment, the mixture was washed briefly with a sodium phosphate buffer (100 mM, pH 8.0) followed by capping of unreacted aldehyde groups at 200 rpm for 30 min using a Tris–HCl buffer (100 mM, pH 8.0). The sample was then washed once with a sodium phosphate buffer (100 mM, pH 8.0), twice by another sodium phosphate buffer (10 mM, pH 6.5), and stored at 4 °C in the buffer (10 mM sodium phosphate, pH 6.5). For an adsorbed sample, fresh phosphate buffer (100 mM, pH 8.0) was used instead of the GA solution.

The amount of protein leaching from the multi-catalyst system into the supernatant was measured by using the BCA (PIERCE, Rockford, IL) method.[20] The final enzyme loading in the multi-catalyst system was calculated from the difference between the

amount of initially added enzyme and the amount in leached solution.

2.5 Preparation of catalyst systems consisting of MNPs covalently (Cov-Gal Ox) or physically (Phy-Gal Ox) immobilized by Gal Ox without silica matrix

For covalent immobilization of Gal Ox on MNPs, amine groups were first modified on MNPs by following the reported procedure.[21] Aminated MNPs (10 mg) were incubated in 1.5 mL of 0.1% GA solution (100 mM sodium phosphate buffer, pH 8.0) for 1 h, and washed five times with the same buffer without GA. The aldehyde-functionalized MNPs were then incubated in Gal Ox solution (6 mg mL^{-1} in 10 mM sodium phosphate buffer, pH 6.5) for 1 h, and subjected to the same procedures as those used for the multi-catalyst. Gal Ox was physically adsorbed on MNPs following the same procedures with Cov-Gal Ox but using free MNPs instead of aldehyde-functionalized MNPs.

2.6 Determination of galactose concentration using the multi-catalyst system

Galactose detection was performed in a single tube by employing the following procedure. The multi-catalyst (12 μL of 20 mg mL^{-1}) and 120 μL of the sample solution were added to 36 μL sodium phosphate buffer (10 mM, pH 6.5) and incubated at 30 °C for 30 min. To this mixture, 24 μL of the colorimetric substrate (60 mM ABTS) and 48 μL of sodium acetate buffer (500 mM, pH 4.0) were added followed by incubation at 40 °C for 10 min. After reaction, the multi-catalyst was removed from the solution by application of a strong external magnetic field for 30 s giving a supernatant that was used to capture color images. The supernatant (100 μL) was diluted with 900 μL of water for the absorption spectroscopy measurement. Spectrophotometric measurements were carried out in a scanning mode or at 417 nm on a Cary 100 Conc UV-Visible spectrophotometer (Varian, CA) equipped with a desktop computer for absorbance data acquisition.

For the assay in a 96 well-plate, a mixture of 9 μL of multi-catalyst (20 mg mL^{-1}) and 90 μL of sample solution in 27 μL sodium phosphate buffer (10 mM, pH 6.5) was incubated at 37 °C for 30 min. Into each well, 18 μL of ABTS (60 mM) and 36 μL of sodium acetate buffer (500 mM, pH 4.0) were added followed by incubation at 37 °C for 10 min. After reaction, the well-plate was subjected to the same procedures as those used in a tube detection using a Microplate reader (Molecular Devices, CA).

The operational stability of the galactose sensing system was checked in aqueous buffer (10 mM sodium phosphate, pH 6.5) at room temperature under non-shaking conditions. The initial and residual activities at each time point were determined by measuring the absorbance at 417 nm as described above. The relative activity (%) was calculated by using the ratio of the residual activity to the initial activity of each sample. Magnetic reusability was measured after iterative cycles involving the typical reaction using ABTS, magnetic capture, and excessive washing (3 times) with aqueous buffer (10 mM sodium phosphate, pH 6.5). The excessively washed sample was reused for the measurement of the residual activity. The relative activity (%) at each cycle point was determined by using the ratio of the retained activity to the initial activity.

2.7 Diagnosis of galactosemia from clinical dried blood spot specimens

A standard curve was first constructed using reference samples prepared by loading 20 μL solutions containing various concentrations of galactose onto a filter paper disk (5/16 in. in diameter, type 2992, Schleicher & Schuell). The filter papers were dried overnight at room temperature and stored in a zippered plastic envelope at 4 °C until use. Blood discs (3 mm diameter) were punched from clinical samples, derived from dried blood specimens of newborns at clinical hospitals. The disks were placed into wells of the 96 well-plate. Artificial galactosemia mimics were prepared by applying 10 μL galactose solution containing higher levels of galactose than cutoff values (80 mg L^{-1}) of galactosemia onto the blood disc (3 mm diameter). The concentrations of galactose in each blood disc equaled the added galactose plus that present in the original blood sample.[12] The galactose concentrations of the blood discs were determined by using an enzymatic galactose assay (Bio-rad, UK) and then by analysis using a Microplate reader (Molecular Devices, CA) according to the manufacturer's instructions and protocols.

The spot specimens (3 mm diameter), including standard, control, artificial galactosemia mimics, and unknown real clinical samples, were placed into the respective wells of the 96 well-plate. To elute galactose adsorbed on the paper, samples were incubated with 3% trichloroacetic acid for 1 h at room temperature with moderate shaking. Then, 30 μL of each eluted solution was transferred into another well and mixed with 60 μL of a mixture comprised of 0.5 mL of sodium bicarbonate (1 M) and 1.5 mL of sodium phosphate (10 mM, pH 6.5). The galactose concentration in each solution (90 μL) was then determined by using the procedure described in Section 2.6.

3. Results and discussion

3.1 Construction of the multi-catalyst system for colorimetric quantification of galactose

The new nanoscale multi-catalyst system for galactose quantification consists of Gal Ox and MNPs, simultaneously entrapped in large pore sized mesocellular silica (Fig. 1). For construction of this system, MNPs were first incorporated in the mesopores of silica by impregnation with $Fe(NO_3)_3 \cdot 9H_2O$ followed by heat treatment at 400 °C under an Ar/H_2 atmosphere. This procedure results in the formation of magnetic mesoporous silica (MMS) containing 40 wt% magnetite to the weight of silica matrix (MMS-40). XRD, DLS, and TEM analyses were performed to gain insight into the structure of MMS-40. The peaks in the XRD pattern of MMS-40 (Fig. S1, ESI†) heat-treated at 400 °C matched those with the standard crystal structure data of MNPs (JCDPS, no. 19-0629) and the size of the MNPs formed within the matrix was determined to be 16 nm, as calculated using the Scherrer equation.[22] Narrow particle size distributions of MMS-40 around 700 nm were observed by the DLS method (Fig. S2, ESI†). As seen in the TEM images

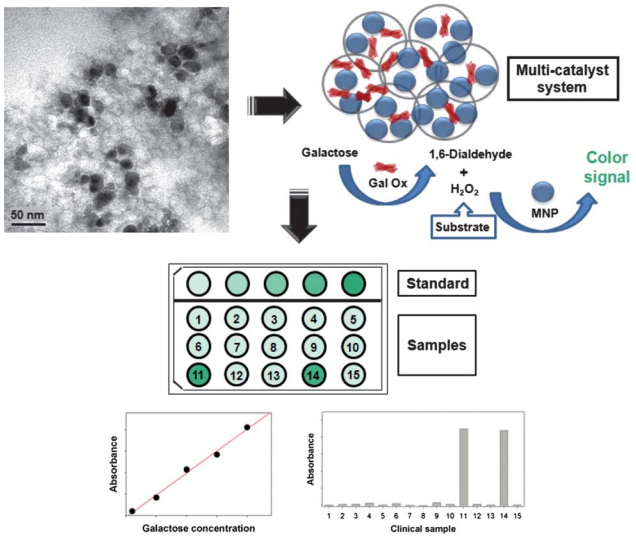

Fig. 1 Schematic illustration of the multi-catalyst system for quantification of galactose, entrapping both MNPs and Gal Ox in mesocellular silica.

(Fig. 1 and S3, ESI†), a high fraction of vacant pores exist in the MMS-40 which are available to accommodate enzyme molecules. Gal Ox was subsequently immobilized in the MMS-40 by employing the cross-linked enzyme aggregate (CLEA) method, which has proven to be effective for preventing enzyme leaching from the matrix.[19,23] A final Gal Ox loading amount after excessive washings was determined to be over 10 wt%, by using a BCA assay.[20] We also examined the effect of different amounts of magnetite and the concomitant enzyme loading on the sensing performance of target molecule using three MMSs with different magnetite loadings (MMS-20, MMS-40, and MMS-60). As the magnetite loading increased to MMS-40 and MMS-60 from MMS-20, the respective Gal Ox loading amount decreased to 11 wt% and 6 wt% from 13 wt%. This is due to the higher pre-occupation of MNPs inside the silica restricting the amount of immobilized Gal Ox. Studies of the colorimetric reaction of ABTS to detect target galactose using multi-catalyst systems prepared from MMS-20, MMS-40, and MMS-60 showed that the multi-catalyst system from MMS-40 has the highest sensing activity even though the differences between the systems were small (Fig. S4, ESI†). The results of these experiments led us to select MMS-40 as a matrix for the immobilization of Gal Ox in further efforts to develop a MMS-based galactose biosensor.

To confirm that Gal Ox molecules are well immobilized inside the mesopores of silica, nitrogen physisorption was carried out on the multi-catalyst system containing Gal Ox and a control consisting of bare MMS without enzyme (Fig. S5, ESI†). By employing this procedure, the BET specific surface area, single point pore volume, and pore size were determined to be 273 m^2 g^{-1}, 1.34 cm^3 g^{-1}, and 38.7 nm, respectively, for MMS without Gal Ox, and 197 m^2 g^{-1}, 1.01 cm^3 g^{-1}, and 32.8 nm, respectively for the MMS containing immobilized Gal Ox (Fig. S5, ESI†). The decrease observed in the three parameters by 15–28% confirms that Gal Ox molecules are located inside the silica pores.

3.2 Analytical capabilities of the multi-catalyst system: specificity, linearity, sensitivity, and precision

We envisioned that the nanostructured material obtained by entrapping Gal Ox in MMS would serve as an efficient colorimetric galactose biosensor system capable of being used for diagnosing galactosemia. In this multi-catalyst system, Gal Ox generated H_2O_2 by catalyzing the oxidation of galactose, which subsequently activates the MNPs to convert a selected substrate into a colored product (Fig. 1). The peroxidase-like activity of MMS-40 was also proven to be higher than that of free MNPs due to the well-dispersed immobilization of MNPs whereas free MNPs are prone to aggregation.[15] To achieve maximal sensing performance of the multi-catalyst system, various reaction parameters including buffer system (pH, composition, and ionic strength), reaction time, and the amount of reagents (multi-catalyst and ABTS) were tested and optimized to find the optimal reaction conditions for the detection of target galactose (Fig. S6, ESI†). We also prepared two other catalyst systems by immobilizing Gal Ox directly onto the MNPs without the silica matrix. For the directly immobilized systems, Gal Ox was covalently immobilized (Cov-Gal Ox) or physically adsorbed (Phy-Gal Ox) on MNPs. The loading capacity of Gal Ox onto the MNPs was below 3 wt% with the two control systems, a value that is much lower than that of the multi-catalyst in MMS-40 (11 wt%). Consequently, the respective volumetric activities of Cov-Gal Ox and Phy-Gal Ox were only 30% (Fig. S7, ESI†), when they were employed in the colorimetric reaction of ABTS to detect target galactose. The results clearly indicate that the silica matrix is essential in order to achieve desired performance of the multi-catalyst system.

The analytical capability of the multi-catalyst system for quantitative detection of galactose in samples was assessed. By utilizing the simple colorimetric reaction and ABTS as the substrate (Experimental), galactose was detected through observation of the development of a vivid color change to green and a corresponding absorption spectral change in 40 min (Fig. 2). In contrast, no significant colorimetric change and absorption band development were observed for negative control samples, such as those containing glucose, arabinose, and fructose. This finding demonstrates that the sensor has excellent specificity only toward galactose. In the case of lactose, however, a considerable signal is detected, which is consistent with the fact that Gal Ox exhibits significant catalytic activity for this carbohydrate.[24] The undesirable reactivity of lactose should not interfere with galactose detection because lactose is efficiently

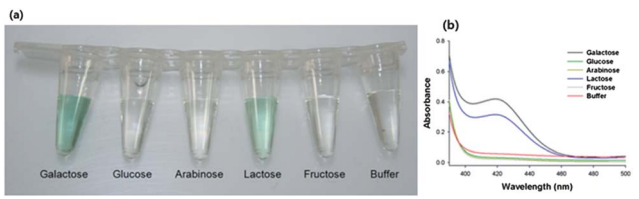

Fig. 2 (a) Photographs of the selective colorimetric detection of galactose using the multi-catalyst system entrapping Gal Ox in MMS-40 and (b) corresponding absorption spectra using ABTS as a substrate. Samples including 5 mM galactose and other control substances such as glucose, arabinose, lactose, and fructose were employed in this experiment.

cleaved to form glucose and galactose by the enzyme lactase found in humans. As a result, lactose does not exist in an appreciable quantity in human blood.[25]

From analysis of a dose–response curve for the multi-catalyst system, the limit of detection (LOD) for galactose was determined to be as low as 5 mg L^{-1} with a linear range from 10–200 mg L^{-1} (Fig. S8, ESI†). The LOD is 10 times lower than those of previously reported enzyme catalysis-based colorimetric detection methods for galactose.[12–14] Considering that the galactose cut-off value in the blood of patients with galactosemia is about 80 mg L^{-1}, the new sensor system is sufficiently sensitive to distinguish between diseased and normal patients. Owing to the fact that in this convenient strategy galactose quantification is associated with generation of a visible color or a spectroscopically detected absorption change, like that employed in a conventional ELISA method, the multi-catalyst system is applicable to a microscale well-plate format with a multiplex analyzing capability. As a result, multiple samples containing galactose at various concentrations were simultaneously analyzed in the same manner based on visible images along with corresponding absorption spectral changes (Fig. 3a and b). The well-plate format also displays excellent linearity in quantification of galactose up to 200 mg L^{-1} (Fig. 3c), an ideal range for diagnosis of galactosemia.

The precision of analysis in a well-plate format was assessed by employing within- and between-analytical assays using several galactose concentrations (50, 100, and 200 mg L^{-1}). For this purpose, the coefficient of variation (CV) and recovery rate ([CV (%) = SD/average × 100] and [recovery (%) = measured value/expected value × 100]) were determined. The within- and between-assay variations were determined by using the results of three parallel experimental set-ups for each sample carried out over a 3 d period. The finding that the within- and between-assay CVs are less than 8% and the recovery rates vary from 99–103% in all experimental datasets show that the expected galactose concentrations can be determined with excellent precision (Table S1, ESI†). All of the results were found to be within an acceptable range when compared with those reported using currently used methods,[9,10,12] ensuring the reliability and reproducibility of this strategy.

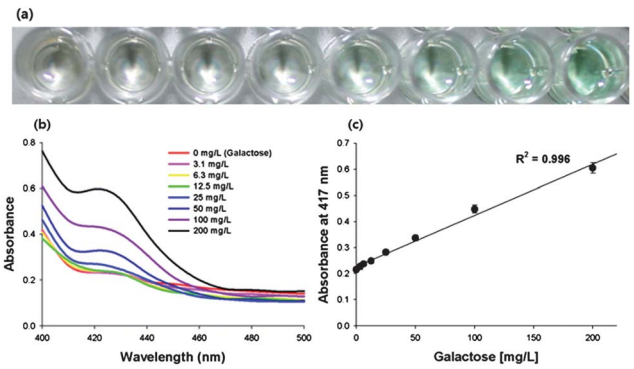

Fig. 3 Linearity of the multi-catalyst system for the quantification of galactose in a well-plate format. (a) Photographs of linear colorimetric detection for galactose and (b) corresponding absorption spectra using ABTS as a substrate. (c) Linear calibration plot. The error bars represent the standard deviations of three independent measurements.

3.3 Magnetic reusability and stability

The new multi-catalyst system was designed to enable easy separation and reuse of the MNPs by employing a simple external magnetic field strategy. The regeneration capability of the multi-catalyst system was assessed and compared with that of the adsorbed Gal Ox in MMS (Ads-Gal Ox) to investigate the effect of CLEA immobilization on the prevention of enzyme leaching from the silica. Magnetic capture of the multi-catalyst system, carried out in a simple and rapid manner, results in capture of the entire system within a 30 s time frame (Fig. 4a). Importantly, the original activity of the system was almost completely retained over 20 iterative cycles. In contrast, the Ads-Gal Ox in MMS lost about 60% of its initial activity after 20 cycles (Fig. 4b) as a consequence mainly of continuous enzyme leaching from the matrix.

The prevention of enzyme leaching achieved by employing the CLEA method also led to enhanced long-term operational stability, as the results in Fig. 4c show. During 20 d operation at room temperature under non-shaking conditions, no significant activity decrease was observed with the multi-catalyst system, whereas Ads-Gal Ox entrapped in MMS and free-Gal Ox in the presence of MMS displayed significant losses of activities (60% and 80%, respectively). We assume that, along with the prevention of the leaching, limited protein unfolding within the confined nanostructure also contributes to this remarkably enhanced stability.[23]

3.4 Diagnosis of galactosemia using clinical blood samples

The most promising application of the new strategy for the quantification of galactose is the diagnosis of galactosemia, one of the metabolic disorders associated with the high levels of galactose in human blood.[1,3,4] Currently, the diagnosis of galactosemia involves the use of special filter paper, which is employed to adsorb a trace amount of blood from the foot of a newborn baby. As a result, we evaluated the clinical

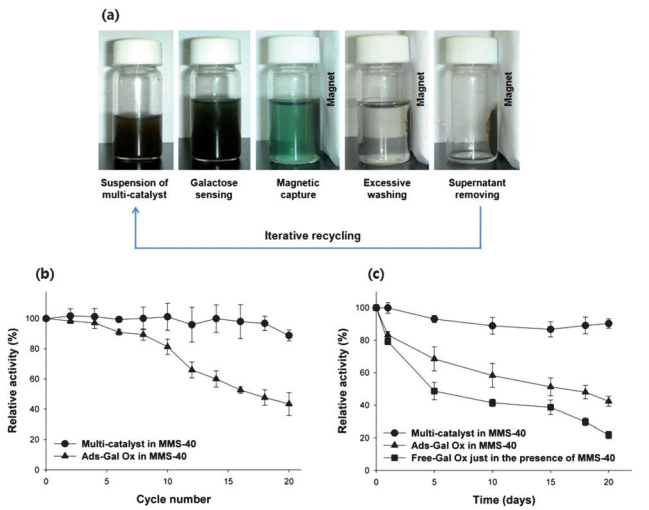

Fig. 4 Magnetic reusability and stability of the multi-catalyst system. (a) Pictures showing that magnetic separation takes place in 30 seconds. (b) Relative activity during 20 iterative cycles of galactose sensing, magnetic capture, and excessive washing using a magnet. (c) Long-term stability.

Table 1 Detection precision of the multi-catalyst assay system in a well-plate format for the determination of galactose levels in dried blood spot specimens

	Sample 1	Sample 2	Sample 3
Expected galactose/mg L^{-1}	24	46	89
Within-assay			
Average[a]/mg L^{-1}	25.0	46.3	90.5
SD[b]	1.52	3.05	3.00
CV[c] (%)	6.1	6.6	3.3
Recovery[d] (%)	104.1	100.7	101.6
Between-assay			
Average/mg L^{-1}	25.3	47.5	90.2
SD	1.42	3.32	3.60
CV (%)	5.6	7.0	4.0
Recovery (%)	105.2	103.3	101.3

[a] Mean of three independent measurements. [b] Standard deviation of three measurements. [c] Coefficient of variation. [d] Measured value/expected value × 100.

applicability of the multi-catalyst system to diagnose galactosemia by determining the concentration of galactose eluted from the dried blood specimens provided by clinical hospitals.

Following the procedures described in Experimental, the concentrations of galactose of three independent blood specimens were determined and their detection precisions were evaluated (Table 1). The within-assay precision was determined from the results of at least three parallel experimental datasets and the between-assay was performed by quantifying galactose for each sample over 3 d. The recovery rates of the within- and between-assays were found to be in the ranges of 100.7–104.1% and 101.3–105.2%, respectively, verifying the excellent precision of the assay system. When compared with currently used methods,[9,10,12] the reproducibility of the new galactose assay system is in an acceptable range as demonstrated by the fact that the CVs of all experimental datasets are less than 7%.

Finally, the diagnostic capability of the new method was utilized to determine normal (24 mg L^{-1}, 74 mg L^{-1}) and patient levels (174 mg L^{-1}, 374 mg L^{-1}) of galactose in blood specimens. Dramatic differences were observed in colorimetric signals for blood specimens derived from normal and patient samples (Fig. 5). In all cases, galactose in the blood specimens were quantified with excellent precisions yielding CVs in a range of 2.5–6.7% and recovery rates from 93–104% (Table S2, ESI†). These observations show that the galactose assay using the multi-catalyst system should serve as a promising analytical tool to diagnose galactosemia in clinical settings.

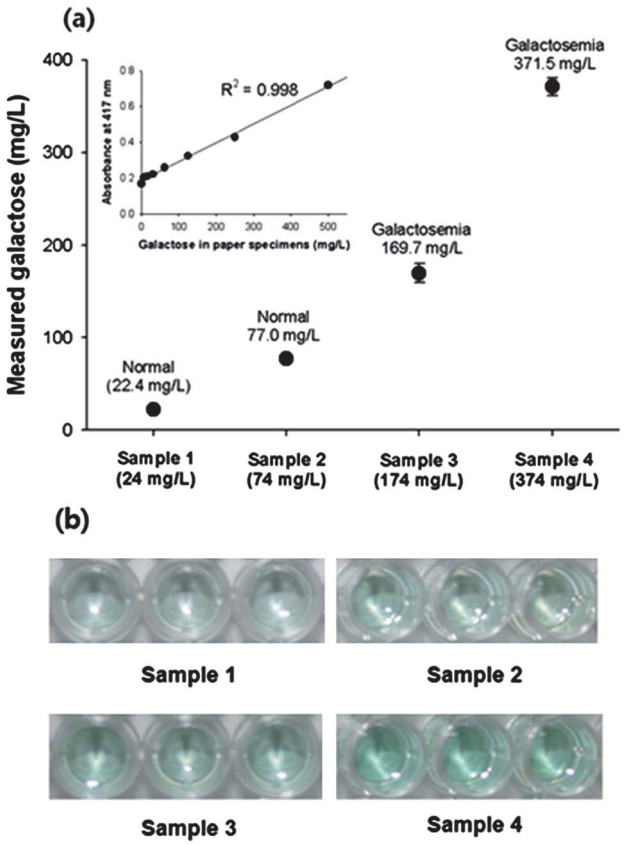

Fig. 5 Colorimetric quantification of galactose in dried blood specimens to diagnose galactosemia. (a) Measurement of different levels of galactose in dried blood specimens representing normal and patients with galactosemia. Inset graph shows the standard curve of the multi-catalyst system for galactose adsorbed on filter paper specimens. (b) Real images showing the colorimetric signal corresponding to each measurement in (a).

4. Conclusions

In the investigation described above, a nanostructured multi-catalyst system, consisting of galactose oxidase and Fe_3O_4 magnetic nanoparticles simultaneously entrapped in large pore sized mesocellular silica, was shown to be an excellent colorimetric sensor to detect and determine the concentrations of galactose. The system displays excellent specificity, linearity, and sensitivity for galactose quantification and it has a high stability along with magnetic reusability. Its use in a well-plate format endows the system with parallel analysis capabilities that were successfully demonstrated by precisely determining galactose concentrations in human dried blood spot specimens. Finally, the multi-catalyst based galactose sensor should serve as a powerful method to detect galactose as part of the diagnosis of galactosemia in newborn babies.

Acknowledgements

This work was supported by the grant from Basic Science Research Program through the National Research Foundation of Korea (NRF) funded by the Ministry of Education, Science and Technology (no. 2009-0080602), NRF Converging Research Center Program (2009-0082276), KRIBB Research Initiative Program, and Business for Cooperative R&D between Industry, Academy, and Research Institute funded Korea Small and Medium Business Administration in 2010 (grants no. 00043279).

Notes and references

1 S. J. Weese, K. Gosnell, P. West and S. S. Gropper, *J. Am. Diet. Assoc.*, 2003, **103**, 373–375.
2 J. S. Jeong, H. R. Yoon and S. P. Hong, *J. Chromatogr., A*, 2007, **1140**, 157–162.
3 G. T. Berry, J. V. Hunter, Z. Wang, S. Dreha, A. Mazur, D. G. Brooks, C. Ning, R. A. Zimmerman and S. Segal, *J. Pediatr.*, 2001, **138**, 260–262.
4 M. Ruiz, S. Jover, M. Armas, M. R. Duque, C. Santana, M. L. Giros and M. D. Boleda, *J. Inherited Metab. Dis.*, 1999, **22**, 943–944.

5 A. F. Winder, P. Fells, R. B. Jones, R. D. Kissun, I. S. Menzies and J. N. Mount, *Br. J. Ophthalmol.*, 1982, **66**, 438–441.
6 R. Guthrie, Human genetics, in *Birth Defects Original Article Series Vol. 4*, ed. D. Bergsma, The National Foundation-March of Dimes, 2nd edn, 1968, pp. 92–97.
7 K. Paigen, F. Pacholec and H. L. Levy, *J. Lab. Clin. Med.*, 1982, **99**, 895–907.
8 O. Y. Hu, T. M. Hu and H. S. Tang, *J. Pharm. Sci.*, 1995, **84**, 231–235.
9 J. S. Jeong, H. J. Kwon, H. R. Yoon, Y. M. Lee, T. Y. Choi and S. P. Hong, *Anal. Biochem.*, 2008, **376**, 200–205.
10 U. G. Jensen, N. J. Brandt, E. Christensen, F. Skovby, B. Norgaard-Pedersen and H. Simonsen, *Clin. Chem.*, 2001, **47**, 1364–1372.
11 S. K. Sharma, Suman, C. S. Pundir, N. Sehgal and A. Kumar, *Sens. Actuators, B*, 2006, **119**, 15–19.
12 F. Diepenbrock, R. Heckler, H. Schickling, T. Engelhard, D. Bock and J. Sander, *Clin. Biochem.*, 1992, **25**, 37–39.
13 Y. Fujimura, S. Ishii, M. Kawamura and H. Naruse, *Anal. Biochem.*, 1981, **117**, 187–195.
14 A. Yamaguchi, M. Fukushi, Y. Mizushima, Y. Shimizu, N. Takasugi, S. Arashima and K. Ohyanagi, *Clin. Chem.*, 1989, **35**, 1962–1964.
15 M. I. Kim, J. Shim, T. Li, J. Lee and H. G. Park, *Chem.–Eur. J.*, 2011, **17**, 10700–10707.
16 L. Gao, J. Zhuang, L. Nie, J. Zhang, Y. Zhang, N. Gu, T. Wang, J. Feng, D. Yang, S. Perrett and X. Yan, *Nat. Nanotechnol.*, 2007, **2**, 577–583.
17 C. Kaittanis, S. Santra and J. M. Perez, *J. Am. Chem. Soc.*, 2009, **131**, 12780–12791.
18 H. Wei and E. Wang, *Anal. Chem.*, 2008, **80**, 2250–2254.
19 J. Lee, J. Kim, J. Kim, H. Jia, M. I. Kim, J. H. Kwak, S. Jin, A. Dohnalkova, H. G. Park, H. N. Chang, P. Wang, J. W. Grate and T. Hyeon, *Small*, 2005, **1**, 744–753.
20 P. K. Smith, R. I. Krohn, G. T. Hermanson, A. K. Mallia, F. H. Gartner, M. D. Provenzano, E. K. Fujimoto, N. M. Goeke, B. J. Olson and D. C. Klenk, *Anal. Biochem.*, 1985, **150**, 76–85.
21 F. Gao, B. F. Pan, W. M. Zheng, L. M. Ao and H. C. Gu, *J. Magn. Magn. Mater.*, 2005, **293**, 48–54.
22 B. D. Cullity and S. R. Stock, *Elements of X-Ray Diffraction*, Prentice-Hall, New York, 3rd edn, 2001, p. 167.
23 M. I. Kim, J. Kim, J. Lee, H. Jia, H. B. Na, J. K. Youn, J. H. Kwak, A. Dohnalkova, J. W. Grate, P. Wang, T. Hyeon, H. G. Park and H. N. Chang, *Biotechnol. Bioeng.*, 2007, **96**, 210–218.
24 G. Avigad, D. Amaral, C. Asensio and B. L. Horecker, *J. Biol. Chem.*, 1962, **237**, 2736–2743.
25 J. D. Ford and J. C. Haworth, *Clin. Chem.*, 1964, **10**, 1002–1006.